ANTIOXIDANTS & REDOX SIGNALING
Volume 00, Number 00, 2019

DOI: 10.1089/ars.2019.7805

Leukocyte Proteomic Profiling in First-Episode Schizophrenia Patients: Does Oxidative Stress Play Central Roles in the Pathophysiology Network of Schizophrenia?

Jie Jiang,[1,2,*] Chao Peng,[3,*] Liya Sun,[1] Jing Li,[4] Ying Qing,[1] Xiaowen Hu,[1] Xuhan Yang,[1] Yan Li,[1] Chuangye Xu,[1] Juan Zhang,[1] Jie Min,[5] Xingwang Li,[1] Shengying Qin,[1] Mei Lin,[6] Liwen Tan,[7] and Chunling Wan[1,2]

Abstract

Although several underlying etiologic implications for schizophrenia (SZ) have been proposed, the cross talk between them is rarely explored systematically. The aim of the present study was to illustrate the pathogenic mechanism of SZ through describing a systematical pathophysiology network using proteomic signatures in first-episode SZ patients. A total of 3152 proteins were identified in leukocytes, and 475 of these proteins were significantly altered in SZ. Functional analysis revealed that cell redox homeostasis was dramatically disrupted, demonstrated as upregulated glycolysis, mitochondrial oxidative phosphorylation, and thioredoxin-centered antioxidant system. We also identified an activated complement system and caspase-independent apoptosis. In addition, increased pyruvate and lactate levels and decreased lactate-to-pyruvate ratios were observed in plasma of SZ patients. The results here lead to the hypothesis that increased oxidative stress is caused by metabolic upregulation and complement activation, which induces protein damage and cell apoptosis, thus contributing to the development of SZ. *Antioxid. Redox Signal.* 00, 000–000.

Keywords: schizophrenia, proteome, oxidative stress, metabolism, immunity

Introduction

As the onset of schizophrenia (SZ) is a result of complex interactions between genetic, developmental, and environmental factors, the pathophysiology of SZ is complicated, and characterizing individual molecules is insufficient. Hence, determining the combined interactions of these molecules using profiling approaches is necessary to better understand SZ.

Genomic studies have provided potential directions, such as immune and energy metabolic dysfunctions, for SZ research but could not determine how gene variations impact the pathophysiology of the disease (7). Proteomic studies, which investigate the abundance, distributions, and functions

[1]Bio-X Institutes, Shanghai Mental Health Center, Shanghai Jiao Tong University, Shanghai, China.
[2]Key Laboratory for the Genetics of Developmental and Neuropsychiatric Disorders (Ministry of Education), Shanghai Key Laboratory of Psychotic Disorders, Shanghai Jiao Tong University, Shanghai, China.
[3]National Facility for Protein Science in Shanghai, Zhangjiang Lab, Shanghai, China.
[4]Department of Bioinformatics and Biostatistics, School of Life Sciences and Biotechnology, Shanghai Jiao Tong University, Shanghai, China.
[5]Mental Health Center, Pudong New Area, Shanghai, China.
[6]Clinical Laboratory, Taizhou People's Hospital Affiliated to Nantong University, Taizhou, China.
[7]Second Xiangya Hospital, Central South University, Changsha, China.
*These authors contributed equally to this article.

Innovation

Many etiology hypotheses are proposed but are still independent for schizophrenia (SZ). We first describe and combine the signatures of energy metabolism, immunity, oxidative stress, and apoptosis that are frequently proposed in the pathophysiology of SZ in a single study, and point the central roles of oxidative stress. We also identify an upregulated thioredoxin-centered antioxidant system on oxidative stress in SZ. This study provides a panoramic proteome profile in first-episode drug-naive SZ patients, which is informative for better understanding of the disease and implicates that antioxidative stress may be future therapeutic directions for SZ.

of total proteins in cells or tissues, may contribute to unraveling biological abnormalities, therefore providing different levels of understanding compared with those provided by genomics. For decades, mass spectrometry (MS)-based proteomic studies conducted in the periphery and brain have allowed investigators to provide more information on the pathophysiology of SZ, including energy metabolism, immune system, mitochondrial dysfunction, oxidative stress, and the cytoskeleton (1, 6). However, due to different antipsychotic drugs, disease stages, and postmortem intervals across samples, the results of these studies are not exactly consistent. Moreover, as a result of the limited number of identified proteins, these studies usually reveal a single biological process and cannot comprehensively characterize SZ.

SZ has been considered a systemic disease, and dysfunctions in the periphery and brain are influenced by each other and can be linked. A recent study discovered that malfunction of the lymphatic vessel system in the central nervous system could be a root cause of neuropsychological diseases through inflammation and immune processes in leukocytes (5). Research on clinical samples could provide supplementary information on the pathophysiology of the disease and better characterize first-onset SZ. Moreover, the label-free ultrahigh-performance liquid chromatography/tandem mass spectrometry (UPLC-MS/MS) method has been proven to have high resolution and sensitivity and can identify thousands of proteins across different samples (2).

In this study, peripheral blood leukocytes from first-episode, drug-naive patients with SZ and healthy controls (HCs) were used to perform this UPLC-MS/MS-based proteomic investigation. Based on the proteomic profiling, we expect to specifically characterize the biological abnormities and propose a potential pathophysiology network for SZ.

Results

Leukocyte proteome profiling

The demographic and clinical information for subjects is shown in Table 1, and no significant difference existed between the two groups. A total of 4136 nonredundant proteins across 16 SZ patients and 10 HCs were identified based on the SwissProt database. Protein abundance in each sample is shown in Figure 1. A total of 2632 ± 139 proteins were identified in each sample, and 1573 proteins were detected covering all 26 samples (Fig. 1A, C). The total protein abundance represented by the total label-free quantification (LFQ) intensity was 13.15 ± 11.95 ($\log_{10}$ transformed, Fig. 1B). After excluding proteins with less than three sample results available in either group, 3152 proteins were left. After statistical analysis, 475 proteins were altered in SZ compared with those in controls ($p < 0.05$, absolute fold change >1.2); among these proteins, 217 were increased, and 258 were decreased (Fig. 1D). SZ patients showed good separation from HCs corresponding to the first two components by principal component analysis (PCA) of differentially expressed proteins (Fig. 1E).

Redox balance, energy metabolism, and immunity are significantly disrupted

The total proteins and altered proteins were distributed in leukocytes globally, and the cytosol, nucleus, membrane, and mitochondrion were the most abundant subcellular localizations (Fig. 2A). When using 3152 total proteins as background

Table 1. Demographic and Clinical Characteristics of Subjects Involved in Proteomic Study and Validation Study

	Proteomic study		*Validation study*	
	SZ	*HC*	*SZ*	*HC*
Total number	20	10	40	40
Male/Female, *N*	8/12	2/8	14/26	12/28
Age, year, mean ± SD	23.25 ± 5.94	24.70 ± 1.35	25.97 ± 7.34	26.40 ± 4.33
Weight, kg, mean ± SD	54.94 ± 9.67	52.5 ± 4.92	57.16 ± 11.38	55.88 ± 9.02
Height, cm, mean ± SD	162.75 ± 6.67	160.00 ± 8.33	162.78 ± 6.83	162.40 ± 8.02
BMI, kg/m^2, mean ± SD	20.63 ± 2.48	20.49 ± 0.75	21.46 ± 3.33	21.07 ± 2.07
Waist circumference, cm, mean ± SD	73.69 ± 5.62	73.80 ± 6.51	77.11 ± 8.85	74.48 ± 8.56
Nonsmoker/Smoker	20/0	10/0	40/0	40/0
Nondrinker/Drinker	20/0	10/0	40/0	40/0
PANSS, score, mean ± SD				
Positive scale	19.50 ± 3.48	/	20.62 ± 5.40	/
Negative scale	21.94 ± 7.64	/	18.97 ± 8.13	/
General psychopathology scale	32.53 ± 6.58	/	32.56 ± 6.17	/
Total	73.31 ± 12.55	/	72.05 ± 11.79	/

BMI, body mass index; HC, healthy control; PANSS, Positive and Negative Syndrome Scale; SD, standard deviation; SZ, schizophrenia.

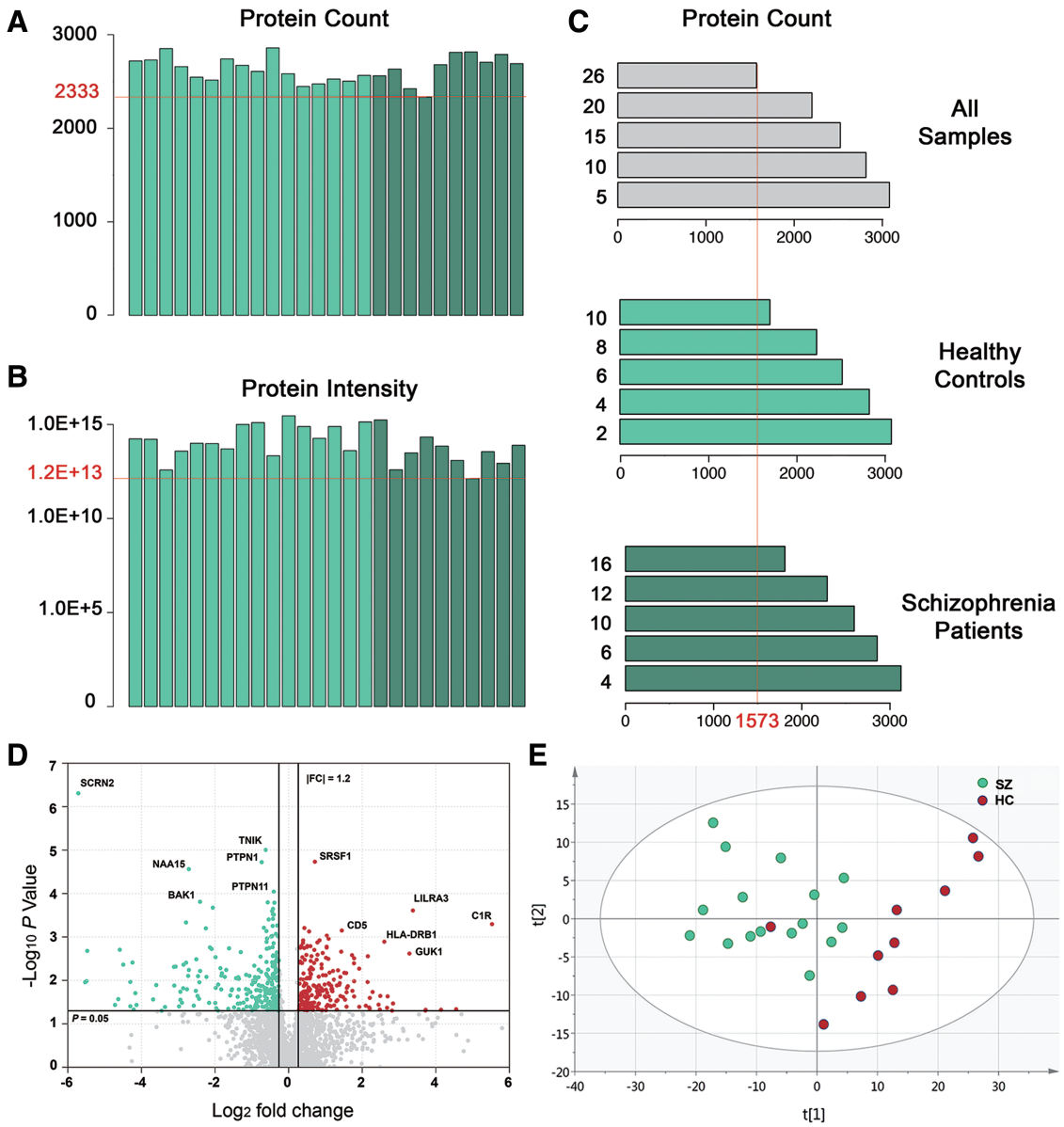

FIG. 1. Proteomic profiling in leukocyte. **(A)** Protein counts detected in 16 patients and 10 healthy controls. **(B)** Protein intensities measured in 16 patients and 10 healthy controls. **(C)** Protein counts detected in different sample sets. **(D)** Volcano plot of all identified proteins. Differentially expressed proteins ($p < 0.05$, absolute fold change >1.2) were highlighted, and several altered proteins are marked. **(E)** PCA of differentially expressed proteins between patients and healthy controls. The first two principal components account for 47.1% of the total variance. PCA, principal component analysis. Color images are available online.

to perform Gene Ontology (GO) analyses, mitochondrion was the only significantly enriched organelle in altered proteins (Fig. 2B). ''Cellular oxidant detoxification,'' ''response to oxidative stress,'' and ''negative regulation of apoptotic process,'' related to mitochondrial functions, were significantly enriched biological processes, and ''peroxidase activity'' was the most significant enriched molecular function (Fig. 2B). These results indicated that mitochondrial functions, especially the cellular redox balance, were greatly altered in leukocytes in SZ.

To further characterize the alterations, we performed GO and pathway analyses on upregulated and downregulated proteins separately. In upregulated proteins, GO terms, including ''mitochondrion,'' ''cell redox homeostasis,'' and ''cellular oxidant detoxification,'' and pathways related to metabolism and immunity were remarkably enriched (Fig. 2C, E). Among enriched pathways, ''carbon metabolism,'' ''oxidative phosphorylation,'' ''TCA cycle,'' and ''pyruvate metabolism'' are related to energy metabolism and mitochondrial functions. ''Complement and coagulation cascades'' was the most significantly altered immune pathway. In contrast to the consistency and aggregation in increased proteins, terms enriched in decreased proteins were diverse, and no terms were related to mitochondrial functions or oxidative stress (Fig. 2D, F).

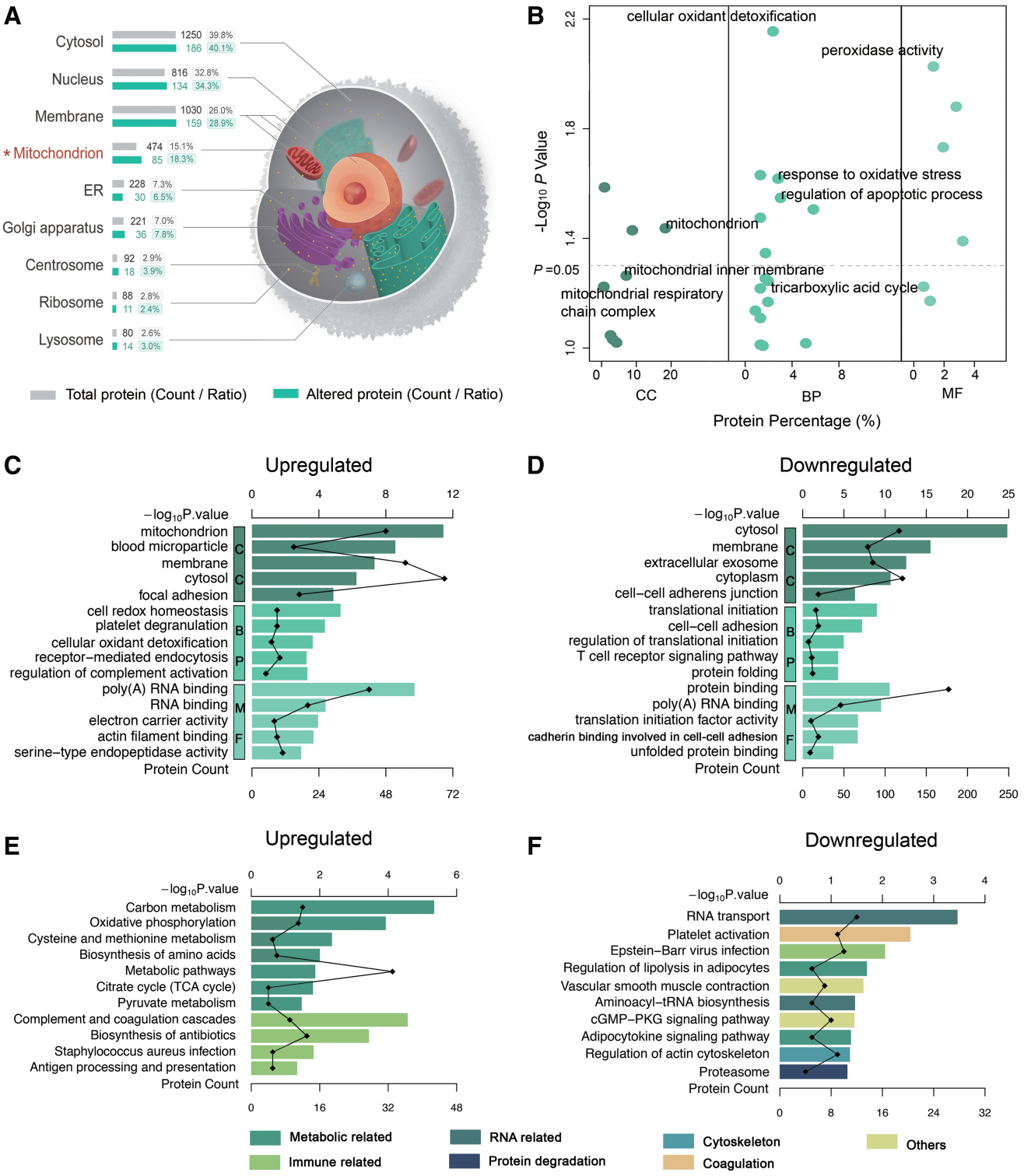

FIG. 2. GO and KEGG pathway analysis of altered proteins. **(A)** Subcellular localizations of total proteins and altered proteins in leukocytes. Protein localizations are performed by CC analysis on DAVID. CC annotations were found for 3088 total proteins and 466 altered proteins. The *gray bars* represent the percentages of the total proteins that are active in the relevant organelle, and the *green bars* represent those of altered proteins. As many proteins function across the cell, the sum of the percentages is >100%. $*p < 0.05$. **(B)** Results of GO analysis on altered proteins using 3152 total proteins as background. **(C–F)** The top 5 significantly enriched GO terms **(C, D)** and all significantly enriched pathways **(E, F)** are demonstrated. Bars represent the $-\log_{10} p$ values, and the points represent protein counts. All pathways are summarized in seven categories. BP, biological process; CC, cellular component; ER, endoplasmic reticulum; GO, Gene Ontology; MF, molecular function. Color images are available online.

Increased oxidative stress, upregulated antioxidant system, and activated apoptosis

The disturbance of cellular redox balance was the most significant alteration in SZ patients revealed by our proteomic data. A number of proteins reportedly sensitive to oxidative stress were significantly altered, such as protein deglycase DJ-1 (PARK7), heat shock protein HSP 90-beta (HSP90AB1), HSP90B, and HSPA4 (Table 2). There are two well-known parallel antioxidant enzymic systems called the glutathione (GSH)- and thioredoxin (Trx)-centered system for reducing oxidative stress. Thioredoxin reductase 1 (TXNRD1), Trx (TXNDC5 and TXNDC17), methionine sulfoxide reductase (MSRA), and peroxiredoxins 4 and 5 (PRDX4 and PRDX5), which are involved in the Trx-centered system, were all increased significantly, while glutathione reductase (GR), glutaredoxins (GLRX, GLRX3, and GLRX5), and glutathione peroxidases (GPX1, GPX3, and GPX4), which are involved in the GSH-centered system, were not altered (Fig. 3 and Table 2). These results indicate increased oxidative stress and biased alterations of the antioxidant system in SZ. Meanwhile, all detected caspases and cytochrome c that involved in programmed cell death were not changed, while apoptosis-inducing factor (AIF), apoptosis inhibitor 5, heat shock 70 kDa protein (HSPA4), and Trxs that involved in oxidative stress-induced cell apoptosis were differentially expressed, suggesting the activation of caspase-independent apoptosis in SZ (Fig. 3).

Upregulated glycolysis and oxidative phosphorylation

Most proteins involved in glycolysis, the tricarboxylic acid (TCA) cycle, and oxidative phosphorylation (OXPHOS) were detected and are shown in Figure 4. In the cytoplasm, three of four altered proteins within glycolysis were significantly increased, including glyceraldehyde-3-phosphate dehydrogenase, phosphoglycerate mutase, and phosphoglycerate kinase. Inside mitochondria, malate dehydrogenase 1 and 2 (MDH1 and MDH2) and isocitrate dehydrogenase 1 (IDH1), which are involved in the TCA cycle, were significantly increased. In OXPHOS, four subunits, including NDUFS5, NDUFS6, NDUFA8, and NDUFV2 in nicotinamide adenine dinucleotide (NADH) dehydrogenase complex, were significantly increased, while only NDUFA4 was decreased. All differentially expressed subunits of the ATP synthase complex exhibited higher expression levels, including ATP5A1, ATP5C1, ATP5I, ATP5O, and ATP5H. These alterations suggested substantial upregulation from glucose oxygenolysis to ATP generation. In addition, we observed significantly increased fatty acid synthase and decreased long-chain-fatty-acid-CoA ligase levels in SZ patients (Fig. 4).

Altered complement activation

Figure 5 demonstrates the specific characteristics of the altered complement system in SZ. A total of 10 components and 10 regulatory proteins were detected within the system. Figure 5A shows globally strong positive correlations among

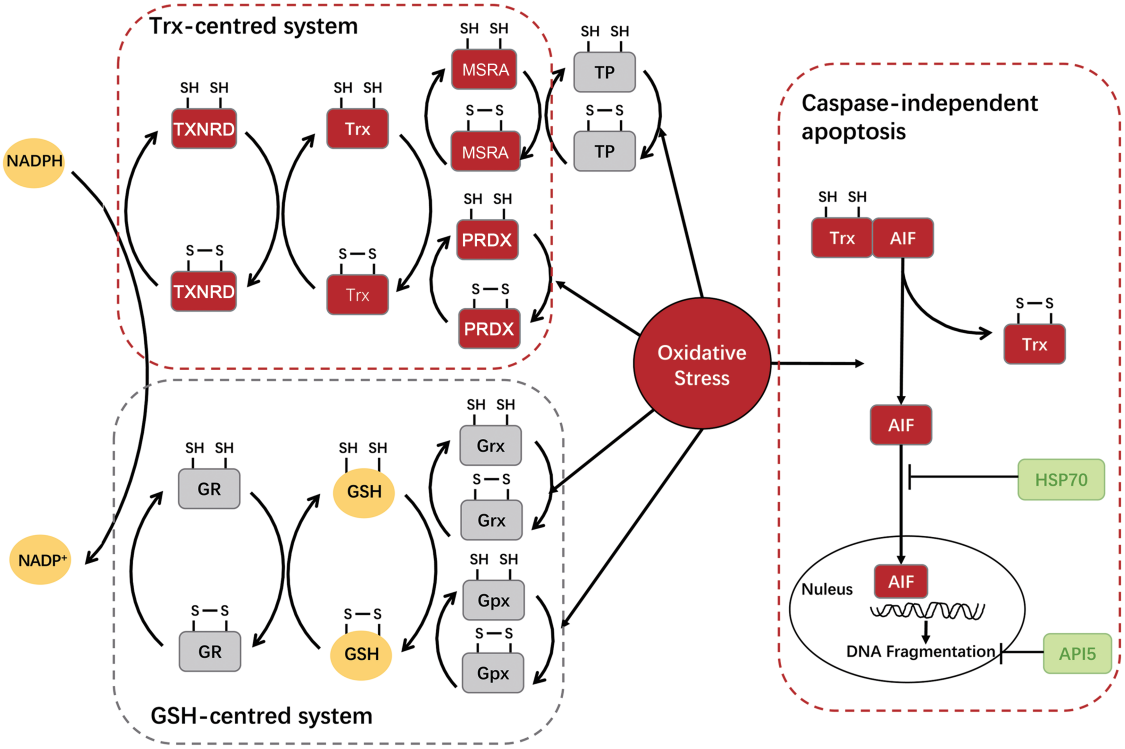

FIG. 3. Altered antioxidant system and increased caspase-independent apoptosis in schizophrenia. The *yellow circles* are metabolites, and the *boxes* are the detected proteins, which are increased (*red*), decreased (*green*), and unchanged (*gray*). Gpx, glutathione peroxidase; GR, glutathione reductase; Grx, glutaredoxin; GSH, glutathione; MSRA, methionine sulfoxide reductase; PRDX, peroxiredoxin; TP, target proteins; Trx, thioredoxin; TXNRD, thioredoxin reductase. Color images are available online.

Table 2. Differentially Expressed Proteins Involved in Oxidative Stress

Accession	*Gene*	*Description*	p	*Fold change*
Q16881	TXNRD1	Thioredoxin reductase 1, cytoplasmic	0.03398	1.27
Q9BRA2	TXNDC17	Thioredoxin domain-containing protein 17	0.03669	2.08
Q8NBS9	TXNDC5	Thioredoxin domain-containing protein 5	0.04020	1.47
P30048	PRDX3	Thioredoxin-dependent peroxide reductase, mitochondrial	0.00567	−1.28
Q13162	PRDX4	Peroxiredoxin-4	0.03333	1.45
P30044	PRDX5	Peroxiredoxin-5, mitochondrial	0.00293	1.29
P05164	MPO	Myeloperoxidase	0.02864	1.28
Q99497	PARK7	Protein deglycase DJ-1	0.00428	1.86
Q8WWN9	IPCEF1	Interactor protein for cytohesin exchange factors 1	0.02672	1.44
P00738	HP	Haptoglobin	0.00110	2.12
O14656	TOR1A	Torsin-1A	0.04165	1.23
P07451	CA3	Carbonic anhydrase 3	0.00961	2.34
Q9UJ68	MSRA	Methionine sulfoxide reductase	0.00334	1.70
P09417	QDPR	Quinoid dihydropteridine reductase	0.01965	1.27
Q99735	MGST2	Microsomal glutathione *S*-transferase 2	0.04687	−18.51
O14880	MGST3	Microsomal glutathione *S*-transferase 3	0.04974	−3.77
P23396	RPS3	40S ribosomal protein S3	0.03357	−1.23
P04264	KRT1	Keratin, type II cytoskeletal 1	0.01496	−1.56
P31749	AKT1	RAC-alpha serine/threonine-protein kinase	0.00021	−4.17
P30519	HMOX2	Heme oxygenase 2	0.02062	−2.20
P23219	PTGS1	Prostaglandin G/H synthase 1	0.02426	−1.21
P08238	HSP90AB1	Heat shock protein HSP 90-beta	0.01354	−1.63
P14625	HSP90B1	Heat shock protein 90 beta family member 1	0.00031	−1.32
P34932	HSPA4	Heat shock 70 kDa protein 4	0.02729	−1.16
Q9Y547	HSPB11	Heat shock protein family B member 11	0.01673	−1.84

these proteins. In detail, seven regulatory proteins, including complement component 1 Q subcomponent binding protein (C1QBP), C4b-binding protein alpha chain (C4BPA), complement factor B, complement factor D, complement factor H (FH), complement factor H-related protein 1, complement factor I (FI), were tightly correlated with each other, and were positively correlated with four complement components, including C1QC, complement C1r subcomponent (C1R), complement C4 (C4) B, and C6. Moreover, complement receptor type 1 (CR1) and CD59 glycoprotein (CD59) were also positively correlated, and were negatively correlated with complement components C8B. These results suggest a tight coexpression network within the complement system. Box plot shows that except for the component C8B, all detected

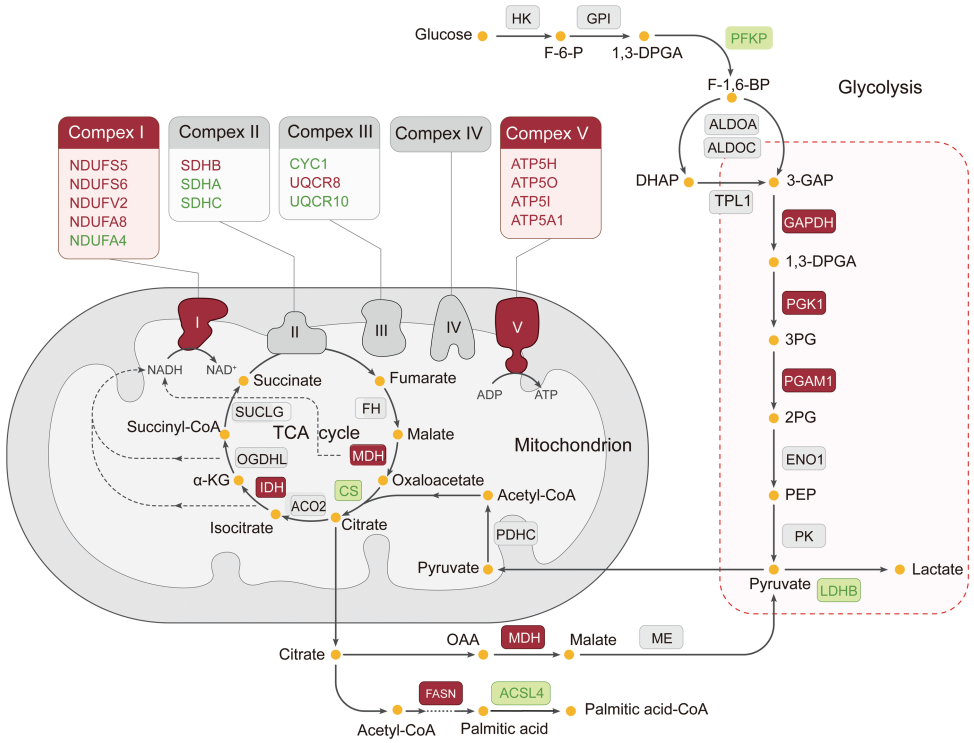

FIG. 4. Upregulated glycolysis and mitochondrial functions. The *yellow circles* are metabolites, and the *boxes* are the detected proteins, which are increased (*red*), decreased (*green*), and unchanged (*gray*). Color images are available online.

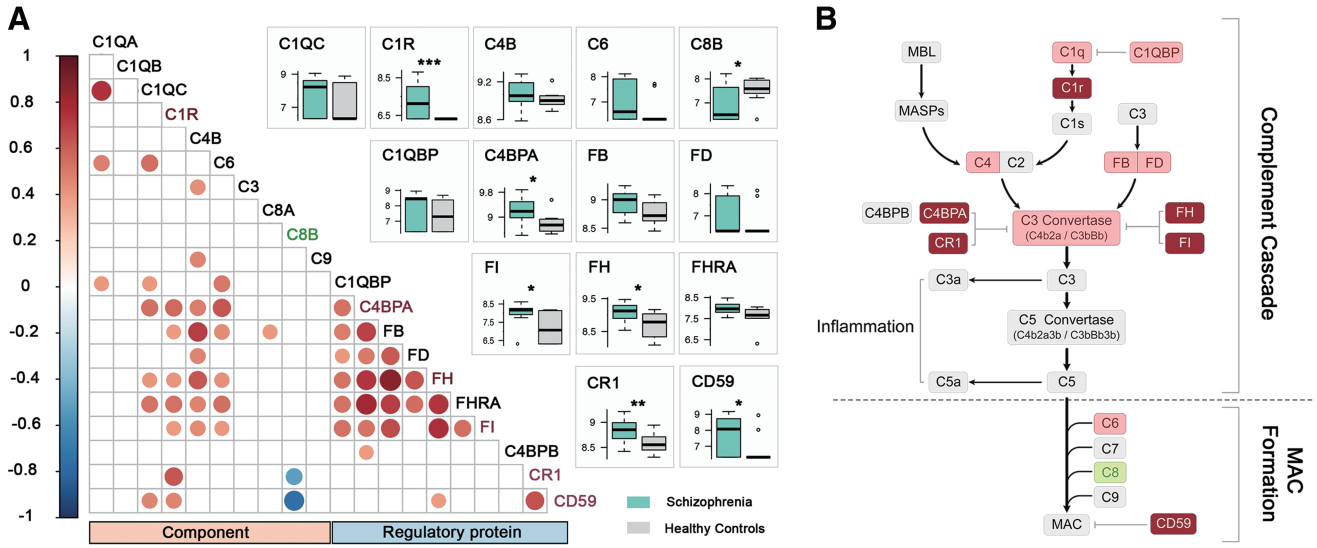

FIG. 5. Altered complement system. (A) Significant correlations ($p<0.05$) across all detected components and regulatory proteins in the complement system are shown. Mean ± standard deviation of abundance ($\log_{10}$ transformed LFQ intensity) of altered proteins between groups are shown in the boxplots. *Green boxes* represent schizophrenia patients and *gray* ones represent the healthy controls. $*p<0.05$; $**p<0.01$; $***p<0.001$. **(B)** The complement activation pathways that consist of complement cascade and MAC formation are shown. Activation is triggered through three pathways that rapidly converge to form a complement C3-cleaving enzyme (C3 convertase, C4b2a, or C3bBb). The C5 convertase (C4b2a3b or C3bBb3b), formed by the recruitment of C3b into the C3 convertase, cleaves C5 to release C5a and C5b. C5b initiates the MAC formation pathway by sequential recruitment of components C6, C7, C8, and C9. C3a and C5a could mediate chronic inflammation. Regulatory proteins, including C1QBP, C4BPA, C4BPB, CR1, FH, FI, and CD59, could inhibit the formation of convertase or MAC. Increased proteins detected in our data (*red*) and speculated by correlation analysis (*light red*) as well as decreased proteins (*green*) are highlighted. C1QBP, complement component 1 Q; C3, complement C3; C4BPA, C4b-binding protein alpha chain; CR1, complement receptor type 1; FH, complement factor H; FI, complement factor I; LFQ, label-free quantification; MAC, membrane attack complex. Color images are available online.

proteins were upregulated in SZ patients. Among these, the upregulation of one complement component C1R and five regulatory proteins, including FH, FI, CR1, C4BPA, and CD59, was statistically significant (Fig. 5A). To explore the implications of these alterations, we mapped these proteins into the complement activation pathways. As shown in Figure 5B, proteins involved in the complement cascade are generally increased, indicating that the complement cascade was initially activated. Meanwhile, the downregulation of C8B and the upregulation of CD59, as well as the negative correlation between the two proteins, imply an impaired membrane attack complex (MAC) formation process in SZ.

Increased plasma pyruvate and lactate levels

We measured the pyruvate and lactate levels in plasma and calculated the lactate-to-pyruvate ratios to confirm the speculated increased glycolysis and mitochondrial function in SZ. Plasma pyruvate and lactate levels were significantly increased by 1.49-fold ($p=0.00034$) and 1.25-fold ($p=0.034$), and the lactate-to-pyruvate ratio was significantly decreased by 1.25-fold ($p=0.0028$) in SZ (Fig. 6).

Discussion

Many glycolytic enzymes and plasma pyruvate levels were increased in our data, suggesting the upregulation of glucose catabolism in SZ. An early proteomic study conducted in peripheral blood mononuclear cells demonstrated the characteristics of glucose metabolism in SZ patients (3). Increased glucose transportor-1 and insulin levels observed in that study suggest elevated glucose consumption in SZ patients, which is consistent with our findings. Due to the application of long-gradient separation coupled with highly sensitive tandem MS, more processes except for glycolysis were illustrated in our study. Increased levels of MDH and IDH indicate that the TCA cycle was upregulated, which is supported by our previous metabolomic study that reported increased citrate, 2-oxoglutarate, and malate levels in SZ patients (9). Eight of the nine altered subunits involved in NADH dehydrogenase and ATP synthase were upregulated, indicating OXPHOS was activated in SZ. In addition, we found significantly decreased lactate-to-pyruvate ratios in SZ patients, indicating the preference for pyruvate production and well-functioning aerobic respiration in the mitochondria of SZ patients. Above all, we speculated that the energy demand and supply are at a high level in leukocytes of first-onset SZ patients (Fig. 7).

The complement system is a key innate immune defense against infection and an important driver of inflammation. This system is associated with SZ on both the gene and protein levels (7, 8). In this study, we identified most proteins involved in the complement system, and most of them were significantly increased, indicating an activated complement cascade pathway. The released complement C3 (C3) a and C5a from the cascade are major mediators of inflammation, which can quickly turn complement from a defense system to an aggressor. Moreover, CD59 could inhibit the formation of

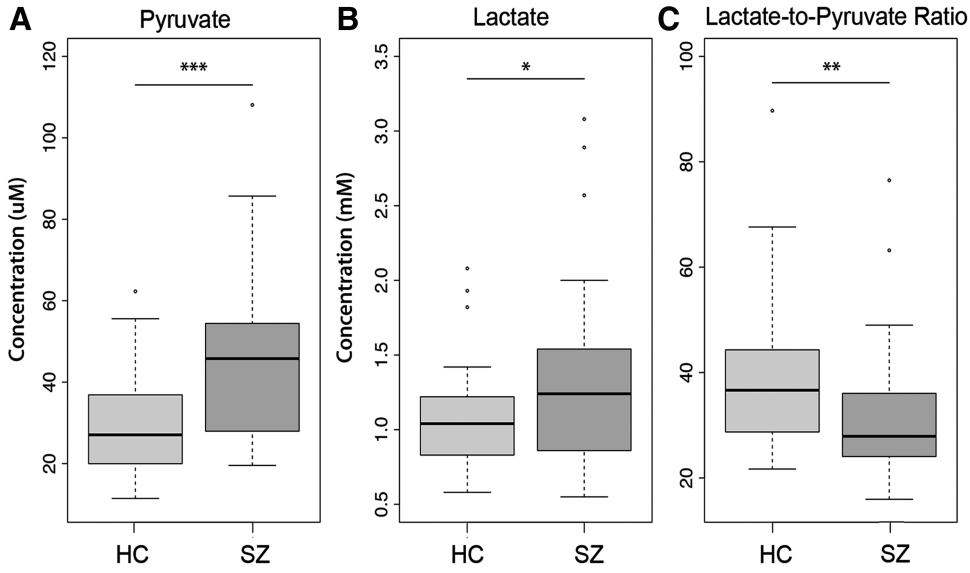

FIG. 6. Plasma metabolite levels in schizophrenia compared with healthy controls. Mean ± standard deviation of **(A)** pyruvate levels, **(B)** lactate levels, and **(C)** lactate-to-pyruvate ratios are shown in boxplots. *$p < 0.05$; **$p < 0.01$; ***$p < 0.001$.

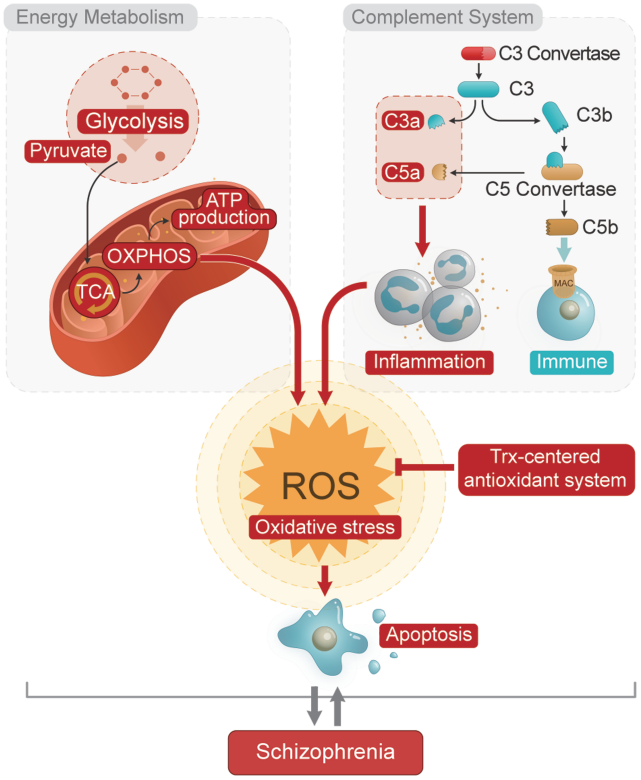

FIG. 7. A proposed pathophysiology network in schizophrenia. In patients with schizophrenia, glycolysis and mitochondrial functions, including the TCA cycle and OXPHOS, are upregulated to satisfy the high energy demand. The complement system downregulates immune functions through MAC but drives inflammation through C3a and C5a. OXPHOS in mitochondria and complement-derived inflammation result in ROS accumulation and increased oxidative stress, in turn inducing protein damage that activates the Trx-centered antioxidant system and cell apoptosis, thus contributing to the development of schizophrenia. OXPHOS, oxidative phosphorylation; ROS, reactive oxygen species; TCA, tricarboxylic acid. Color images are available online.

MAC by competitive binding to C8, so significantly decreased C8B and the negative correlation between CD59 and C8B indicate an impaired MAC function in SZ. Above all, we speculated that the complement system downregulates the functions of the immune response through MAC but causes increased inflammation in SZ (Fig. 7).

The upregulated energy metabolism and inflammation response could induce oxidative stress in cells. Cells need to maintain an adequate intracellular redox balance through antioxidant defense to function properly. Most proteins involved in or functioning with the Trx system were significantly increased, while the GSH system was not altered in SZ, as revealed in this study. The GSH system is more effective in reducing small molecules and reacting directly with reactive oxygen species, whereas Trx is more effective in reducing the oxidized proteins. A great number of studies have reported the alterations of peroxiredoxins in SZ (6), but the deeper mechanisms are rare mentioned. The consistent upregulation of Trx system in this study suggests that increased oxidative stress may induce vast protein damages in cells, and followed by the activation of Trx-centered antioxidant system in SZ. However, continual stress cannot be totally suppressed, so that cell apoptosis was induced. AIF, which is normally localized in mitochondria, translocates to the nucleus to trigger chromatin condensation and DNA fragmentation on oxidative stress through Trx-AIF and HPS70-AIF interactions. The alterations of these proteins, as well as unaltered cytochrome c and caspase 9, strongly support the activation of caspase-independent apoptosis in SZ (Fig. 7). In addition, elevated plasma cell-free DNA levels and apoptotic-like DNA fragmentations were found in our recently published study, which strongly support the activated apoptosis in SZ.

Mitochondria, metabolism, inflammation, and redox mechanisms are proposed to be at the center of SZ etiology, integrating genetic and environmental factors early in neurodevelopment and contributing to the onset of psychosis (1, 4, 7). Our data systematically described the detailed alterations of these aspects at the proteomic level, which not only support the genetic findings but also combine the existing

hypotheses into an associated network (Fig. 7). We also raise a new hypothesis that oxidative stress, induced by alterations of OXPHOS in mitochondria and complement system, will induce protein damage and cell apoptosis, and may converge to cause impaired neurodevelopment and the development of SZ in early life. Moreover, as multiple antipsychotic drugs have good antioxidant properties (4), the results in this study indicate that oxidative stress may be developed as a new therapeutic direction in future treatment.

Notes

Subjects

A total of 40 patients diagnosed with SZ according to the DSM-IV were recruited from the Second Xiangya Hospital of Central South University in Changsha, China. All patients were experiencing their first episode of SZ and were antipsychotic drug naive. Forty HCs with matched age, gender, waist circumference, and body mass index (BMI) were also recruited from Changsha. Of these participants, 20 patients and 10 HCs were included in the proteomic study, and all participants were included in the validation study. All participants had no other physical diseases or drug abuse history and were nonsmokers. Positive and Negative Syndrome Scale ratings were completed through face-to-face interviews with trained raters to determine psychiatric symptom severity. The study was conducted in accordance with the Declaration of Helsinki, and informed consent was obtained after an explanation of the study was provided. The study was approved by the Committee of Human Genetic Resources in Bio-X Institutes at Shanghai Jiao Tong University.

Isolation of plasma and leukocyte total protein from whole blood samples

Five milliliters of EDTA-anticoagulated peripheral blood was collected early in the morning after an overnight fast. Plasma was isolated from 2 mL of fresh blood by centrifugation at 1600 *g* at 4°C for 10 min. Red blood lysis buffer (RT122; Tiangen Biotech Co., Beijing, China) was used to obtain clean leukocytes from another 2 mL of fresh blood by centrifuging at 400 *g* at 4°C for 10 min. TRIzol® Reagent (15596026; Invitrogen Co., Carlsbad, CA) and chloroform were used to separate RNA, DNA, and proteins. After removing RNA and DNA, total proteins were precipitated overnight at −20°C with five volumes of a solution containing ethanol, acetone, and acetic acid (50/50/0.1, v/v/v) and washed by acetone by centrifugation at 14,000 *g* for 1 h at 4°C. The protein was then redissolved in 100 μL 8 *M* urea. After Bradford quantification of protein, total protein staining was performed on sodium dodecyl sulfate-polyacrylamide gel electrophoresis by SYPRO Ruby (S12000; Thermo Scientific, Waltham).

Trypsin digestion

Two hundred micrograms of protein was reduced with 20 m*M* dithiothreitol at 56°C for 1 h, followed by alkylation with 90 m*M* iodoacetamide for 40 min at room temperature in the dark. The protein solution was then ultrafiltered three times by a 10 kDa ultrafiltration tube (VN01H02; Sartorius Co., Gottingen, Germany) and digested with Trypsin at 1:50 (w/w) (V5111; Promega Co., Madison). Peptide products were collected by centrifugation at 14,000 *g* at 4°C for 20 min followed by washing with 50 μL 50 m*M* NH_4HCO_3. The digestion was stopped by acidification with formic acid to obtain a final solution with pH <3. All peptide samples were dehydrated using a vacuum centrifuge and dissolved in 0.1% formic acid before MS analysis.

Label-free protein quantitation by MS

Five micrograms of the digest was desalted and injected in an in-house-made column (C18, 100 μm OD × 360 μm ID, 3 μm 5 μ*M* particle size, 100 Å pore diameter) connected to an Easy LC 1000 system using a 240-min gradient as follows: from 0% to 5% solvent B in 15 min, followed by 5% to 35% solvent B in 200 min, and 35% to 100% solvent B (buffer A: 0.1% formic acid in water; buffer B: 0.1% formic acid in acetonitrile) at a flow rate of 300 nL/min. Eluted peptides were ionized and introduced into a Q Exactive hybrid quadrupole-orbitrap mass spectrometer (Thermo Scientific) using a nanospray source. The MS instrument was operated in data-dependent acquisition mode with automatic switching between MS and MS/MS scans. Full MS scans were acquired at a resolution of 70,000, with an automatic gain control target value of 3×10^6 ions or a maximum injection time of 50 ms within the scan range of 300–1800 *m/z*. Peptide fragmentation was performed by higher energy collision dissociation with normalized collision energy set to 27. The MS/MS spectra of the 20 most abundant ions (top 20 method) were acquired at a resolution of $R = 17{,}500$, an automatic gain control target value of 1×10^5 ions, or a maximum fragment accumulation time of 100 ms.

Data processing

Generation of raw files into MS/MS peak lists and quantifications were performed with MaxQuant software version v1.4.0.8. MS/MS spectra were searched by the Andromeda search engine against the SwissProt Human database (5/25/2015, 20,198 sequences) at a false discovery cutoff ≤1%. Oxidations (M) and acetylation (protein N term) were specified as variable modifications, and carbamidomethyl (C) was specified as fixed modification. A database search was performed with a mass tolerance of 20 ppm for precursor ions for mass calibration. Six amino acids were required as the minimum peptide length. Proteins with at least two peptides (at least one is unique) were considered reliably identified. The database was supplemented with additional sequences for common contaminants and reversed sequences of each entry to aid in the control of false positives. The MS proteomic data have been deposited in the Proteome Xchange Consortium *via* the PRIDE partner repository with the data set identifier PXD011140. LFQ intensity was used as relative quantification of protein. For MS data, proteins with a minimum of three valid LFQ intensities in either group were included in the following data processing workflow. Signals that were originally zero were imputed with the minimum value of all LFQ intensities across samples. All intensities were transformed to a $\log_{10}$ scale after quantile normalization, which was used to ensure that every sample had a peptide intensity histogram of the same scale, location, and shape.

Validation experiments

Plasma isolated from all participants was used to investigate metabolite levels. We used 50 and 5 μL plasma to measure pyruvate and lactate levels, respectively, using the

Pyruvate Assay Kit (ab65342; Abcam, Cambridge, United Kingdom) and L-Lactate Assay Kit (ab65331; Abcam).

Statistical analysis

Logistic regression analysis was conducted for group comparisons and to adjust for confounding factors, including age, gender, BMI, and smoking and drinking habits, using in-house programs written in the R language. Spearman's correlation analysis was used to determine the correlation between proteins. A p value of <0.05 was considered statistically significant. PCA was performed using SIMCA-P 14 (Umetrics). GO and pathway analyses were performed on DAVID database.

Acknowledgments

This work was supported by the National Key R&D Program of China (2016YFC1306900, 2016YFC1306802), the National Natural Science Foundation of China (81771440, 31500667, 81571797), Grants of Shanghai Brain-Intelligence Project from STCSM (16JC1420500), Translational Medicine Funding of Shanghai Jiao Tong University (ZH2018ZDA40), Shanghai Key Laboratory of Psychotic Disorders (13dz2260500), and the Chinese Academy of Science Key Technology Talent Program. All authors report no biomedical financial interests or potential conflicts of interest.

References

1. Davalieva K, Maleva Kostovska I, and Dwork AJ. Proteomics research in schizophrenia. *Front Cell Neurosci* 10: 18, 2016.
2. Distler U, Kuharev J, Navarro P, and Tenzer S. Label-free quantification in ion mobility–enhanced data-independent acquisition proteomics. *Nat Protoc* 11: 795, 2016.
3. Herberth M, Koethe D, Cheng T, Krzyszton N, Schoeffmann S, Guest P, Rahmoune H, Harris L, Kranaster L, and Leweke F. Impaired glycolytic response in peripheral blood mononuclear cells of first-onset antipsychotic-naive schizophrenia patients. *Mol Psychiatry* 16: 848, 2011.
4. Kim Y, Vadodaria KC, Lenkei Z, Kato T, Gage FH, Marchetto MC, and Santos R. Mitochondria, Metabolism, and Redox Mechanisms in Psychiatric Disorders. *Antioxid Redox Signal* 2018. [Epub ahead of print]; DOI: 10.1089/ars.2018.7606.
5. Louveau A, Smirnov I, Keyes TJ, Eccles JD, Rouhani SJ, Peske JD, Derecki NC, Castle D, Mandell JW, and Lee KS. Structural and functional features of central nervous system lymphatic vessels. *Nature* 523: 337, 2015.
6. Martins-de-Souza D, Harris LW, Guest PC, and Bahn S. The role of energy metabolism dysfunction and oxidative stress in schizophrenia revealed by proteomics. *Antioxid Redox Signal* 15: 2067–2079, 2011.
7. Ripke S, Neale BM, Corvin A, Walters JT, Farh K-H, Holmans PA, Lee P, Bulik-Sullivan B, Collier DA, and Huang H. Biological insights from 108 schizophrenia-associated genetic loci. *Nature* 511: 421, 2014.
8. Sekar A, Bialas AR, De Rivera H, Davis A, Hammond TR, Kamitaki N, Tooley K, Presumey J, Baum M, and Van Doren V. Schizophrenia risk from complex variation of complement component 4. *Nature* 530: 177, 2016.
9. Yang J, Chen T, Sun L, Zhao Z, Qi X, Zhou K, Cao Y, Wang X, Qiu Y, and Su M. Potential metabolite markers of schizophrenia. *Mol Psychiatry* 18: 67, 2013.

Address correspondence to:
Prof. Chunling Wan
Bio-X Institutes
Shanghai Jiao Tong University
No. 1954, Huashan Road
Shanghai 200030
China

E-mail: clwan@sjtu.edu.cn

Date of first submission to ARS Central, May 17, 2019; date of acceptance, May 23, 2019.

Abbreviations Used

AIF = apoptosis-inducing factor
BMI = body mass index
C1QBP = complement component 1 Q subcomponent binding protein
C1R = complement C1r subcomponent
C3 = complement C3
C4 = complement C4
C4BPA = C4b-binding protein alpha chain
CD59 = CD59 glycoprotein
CFHR1 = complement factor H-related protein 1
CR1 = complement receptor type 1
FB = complement factor B
FD = complement factor D
FH = complement factor H
FI = complement factor I
GLRX = glutaredoxin
GO = Gene Ontology
GPX = glutathione peroxidase
GR = glutathione reductase
GSH = glutathione
HC = healthy controls
HSPA4 = heat shock 70kDa protein 4
IDH = isocitrate dehydrogenase
LFQ = label-free quantification
MAC = membrane attack complex
MDH = malate dehydrogenase
MS = mass spectrometry
MSRA = methionine sulfoxide reductase
NADH = nicotinamide adenine dinucleotide
OXPHOS = oxidative phosphorylation
PCA = principal component analysis
PRDX = peroxiredoxin
SZ = schizophrenia
TCA = tricarboxylic acid
Trx = thioredoxin
UPLC-MS/MS = ultrahigh-performance liquid chromatography/tandem mass spectrometry